In situ mountain-wave polar stratospheric cloud measurements: Implications for nitric acid trihydrate formation

Christiane Voigt,[1,2,3] Niels Larsen,[2] Terry Deshler,[4] Chris Kröger,[4] Jochen Schreiner,[1] Konrad Mauersberger,[1] Beiping Luo,[3] Alberto Adriani,[5] Francesco Cairo,[5] Guido Di Donfrancesco,[5,6] Joelle Ovarlez,[7] Henri Ovarlez,[7] Andreas Dörnbrack,[8] Bjørn Knudsen,[2] and Jim Rosen[4]

Received 6 August 2001; revised 21 May 2002; accepted 25 July 2002; published 19 February 2003.

[1] Particle size distribution, composition, and optical properties of polar stratospheric clouds (PSCs) have been measured above northern Scandinavia during a nocturnal balloon flight within the polar vortex on 19 January 2000. The mountain-wave PSC mainly consisted of nitric acid trihydrate (NAT) particles with number densities between 0.01 and 0.2 cm^{-3}, median radii of 1 to 2 μm and volumes up to 1 $\mu m^3 cm^{-3}$. A comparison between optical PSC data and optical simulations based on the measured particle size distribution indicates that the NAT particles were aspherical with an aspect ratio of 0.5. The NAT particle properties have been compared to another PSC observation on 25 January 2000, where NAT particle number densities were about an order of magnitude higher. In both cases, microphysical modeling indicates that the NAT particles have formed on ice particles in the mountain-wave events. Differences in the NAT particle number density can be explained by the meteorological conditions. We suggest that the higher NAT number density on 25 January can be caused by stronger wave activity observed on that day, larger cooling rates and therefore higher NAT supersaturation. *INDEX TERMS:* 0305 Atmospheric Composition and Structure: Aerosols and particles (0345, 4801); 0320 Atmospheric Composition and Structure: Cloud physics and chemistry; 0340 Atmospheric Composition and Structure: Middle atmosphere—composition and chemistry; *KEYWORDS:* polar stratospheric cloud (PSC), nitric acid trihydrate (NAT), ozone, gravity wave, PSC formation

Citation: Voigt, C., et al., In situ mountain-wave polar stratospheric cloud measurements: Implications for nitric acid trihydrate formation, *J. Geophys. Res.*, *108*(D5), 8331, doi:10.1029/2001JD001185, 2003.

1. Introduction

[2] Polar stratospheric clouds play a crucial role in ozone chemistry: heterogeneous reactions on PSC particles process halogen species of mainly anthropogenic origin as prerequisite for rapid polar ozone destruction [*Solomon et al.*, 1986]. The heterogeneous reaction rates depend on volume, phase and composition of the PSCs [*Hanson and Ravishankara*, 1993]. Sedimentation of large PSC particles can irreversibly remove reactive nitrogen from the stratosphere [*Waibel et al.*, 1999; *Fahey et al.*, 2001], thereby ruling out a natural path for active chlorine to be recaptured in a stable halogen reservoir.

[3] In situ investigations of PSCs up to altitudes of 25 to 30 km requires a balloon carried platform. Microphysical, optical and chemical PSC particle properties have simultaneously been measured during two flights performed as part of the European-American SOLVE/THESEO 2000 campaign in January 2000. The instrumentation on both flights consisted of the following: particle number density, volume and size distribution of optically detectable particles ($0.15 < r < 10$ μm) and the number density of condensation nuclei (CN, $r > 0.01$ μm) have been measured with three optical particle counters (OPCs) [*Deshler et al.*, 2000]. Particle composition and size has been detected with an aerosol composition mass spectrometer (ACMS) [*Schreiner et al.*, 1999; *Voigt et al.*, 2000a]. Particle backscatter and depolarization at wavelengths of 480, 685, and 940 nm have been measured with two backscatter sondes [*Rosen and Kjome*, 1991; *Adriani et al.*, 1998]. Finally, water vapor has been detected with a frost point hygrometer [*Ovarlez and Ovarlez*, 1994]. Together with accurate temperature data, these measurements provide a unique set of PSC data, which can be used for testing optical models or theories of PSC formation. Much is known about the conditions under

[1]Max-Planck-Institute for Nuclear Physics, Division of Atmospheric Physics, Heidelberg, Germany.
[2]Danish Meteorological Institute, Division of Middle Atmospheric Research, Copenhagen, Denmark.
[3]Eidgenössische Technische Hochschule, Institute for Atmospheric and Climate Science (IACETH), Zurich, Switzerland.
[4]University of Wyoming, Department of Atmospheric Science, Laramie, Wyoming, USA.
[5]Istituto per la Scienza dell'Atmosfera e del Clima, Roma, Italy.
[6]Istituto per la Scienza dell'Atmosfera e del Clima, ENEA-CLIM, Casaccia, Roma, Italy.
[7]Laboratoire de Meteorologie Dynamique, Palaiseau, France.
[8]Institut für Physi2k der Atmosphäre, DLR Oberpfaffenhofen, Wessling, Germany.

0148-0227/03/2001JD001185$09.00

which supercooled ternary solution particles (STS) or ice form [*Carslaw et al.*, 1994; *Schreiner et al.*, 1999; *Voigt et al.*, 2000b; *Koop et al.*, 2000]. In contrast, NAT particle formation and occurrence in the stratosphere is still under debate [*Fahey et al.*, 2001; *Fueglistaler et al.*, 2002; *Dhaniyala et al.*, 2002].

[4] Measurements in two mountain-wave PSCs encountered on 19 January and 25 January 2000 over Scandinavia will be presented, with the emphasis here on 19 January. The mountain-wave PSC observed during the night of 25/26 January was first described by *Voigt et al.* [2000a] and in more detail in the accompanying papers by *Schreiner et al.* [2002] and *Larsen et al.* [2002]. In this paper, simultaneous detection of particle size distribution and optical particle properties are compared to optical model results. A microphysical model is used to simulate NAT particle formation. The impact of large-scale low temperatures on the observed mountain-wave PSCs is discussed. The PSC data sets of both flights are compared and differences in the NAT particle number densities are related to different meteorological conditions of particle formation.

2. Measurements on 19 January 2000

[5] Figure 1 shows the measurement of a PSC extending over a large altitude range between 450 and 570 K potential temperature (20 to 24 km) at temperatures 3 K above to 4 K below T_{NAT}, assuming a mixing ratio of 8 ppbv HNO_3 inside the vortex. The elevated depolarization on the first ascent supports the presence of solid particles in most of the PSC layers (Figure 1e). The depolarization measurement failed after turnaround. Although conditioning effects in the ACMS prevented the determination of particle composition during the first ascent, a water to nitric acid mole ratio of 3.7 (±1.7) measured during the following descent together with the temperature range of the PSC and the elevated depolarization supports the assumption of the presence of NAT particles in most of the PSC layers. Although nitric acid dihydrate (NAD) particle compositions [*Worsnop et al.*, 1993] would still be consistent with the ACMS measurements within the experimental error, the PSC temperatures exceed the NAD equilibrium temperature by up to 5.3 K. Therefore we believe that the particles were composed of NAT.

[6] The observed total particle volume in the PSC ranges between 0.1 and 2 $\mu m^3 cm^{-3}$ (black line in Figure 1b), with an error of 40%. The median radii of the large mode of the particle size distribution (green line in Figure 1b) were found between 1 and 2 μm at number densities between 0.01 and 0.2 cm^{-3} (red line). Particle sizes were also derived from the particle water measurements of the mass spectrometer. Using calibration data, the water count rate (blue dots in Figure 1c) has been converted into a number of water molecules per particle, from which a NAT particle radius has been calculated assuming spherical particles (black squares in Figure 1c). Particle radii were between 0.7 and 1.3 μm. The discrepancy of both data sets can be caused by a reduced sampling efficiency of the aerodynamic lens of the ACMS for particles larger than 1 μm. The nitric acid data are shown in Figure 1d and the optical backscatter data in Figure 1e. The color index is the ratio between the backscatter ratios at 940 and 480 nm. Consistent with the depolarization and the particle size distribution measurements, a color index larger than 8 indicates the presence of a large mode in the particle size distribution, probably solid particles.

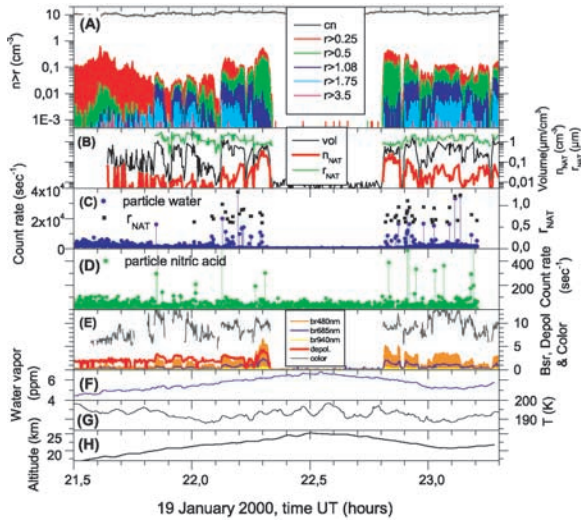

Figure 1. Chemical, microphysical and optical properties of PSCs measured on 19 January 2000 with balloonborne instrumentation. (a) Integrated particle number densities in different size classes N(>r), number density of condensation nuclei (gray line). (b) Total volume (black line), median radius of the large particle mode (green line), number density of the large particle mode (red line). (c) Count rate for condensed phase water (blue dots), particle radius inferred from the measurements (black squares). (d) Count rate for condensed phase nitric acid. (e) Backscatter ratio at 480, 685 and 940 nm wavelengths, depolarization (red line) and color index (gray line). (f) Water vapor mixing ratio. (g) Temperature. (h) Altitude.

3. Combination of Microphysical and Optical PSC Data

[7] Figure 2 shows the backscatter ratio at 685 nm versus temperature. A clear onset in the increase in backscatter at 195 K coincides with temperatures falling below T_{NAT} for the measured water vapor and an assumed HNO_3 mixing ratio of 8 ppbv. High backscatter ratios result from large particle surface areas in the PSC, which have been measured by the OPC and are shown in the lower panel.

[8] The measured particle size distribution has been used as input to an optical model and backscatter ratios at different wavelengths are calculated. The optical simulations are performed with the refractive index for STS particles using the model of *Krieger et al.* [2000] and the scattering matrix calculated by the Mie scheme for the two smallest measured particle size bins ($r < 0.25\mu m$). Larger particles are assumed to consist of NAT with an refractive index of 1.48 and the T-matrix method is used to calculate the backscatter ratios [*Mishchenko*, 1991]. The aspect ratio, i.e., the ratio between the two axes of the solid spheroids, is varied between 0.5 (prolate, cigar-shaped particle) and 1 (spherical particle) in steps of 0.05. A good agreement between the model results and the optical measurements

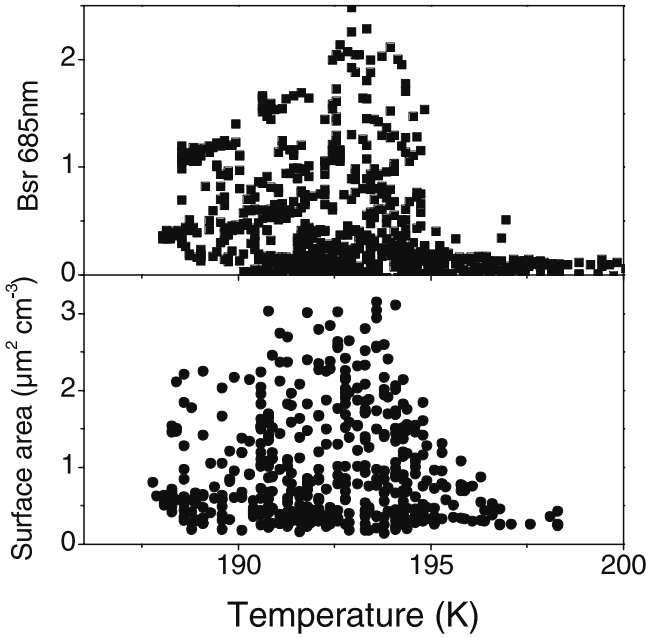

Figure 2. Backscatter ratio at 685 nm versus temperature. Particle surface areas (a > 0.2 $\mu m^2 cm^{-3}$) are shown in the lower panel.

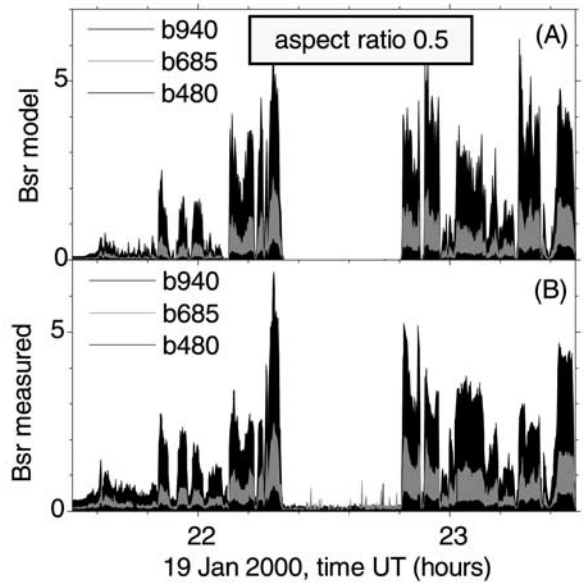

Figure 3. Comparison of backscatter measurements with optical model results. Calculations are performed with an aspect ratio of 0.5 and a refractive index of 1.48 for NAT particles.

at 480, 685 and 940 nm wavelengths could only be achieved using an aspect ratio of 0.5 as shown in Figure 3. Larger aspect ratios lead to higher simulated backscatter ratios and less of an agreement with the measurements. Aspect ratios between 0.5 and 0.7 are still consistent with the measurements within the experimental uncertainty of the OPC [*Deshler et al.*, 2000].

[9] Sensitivity studies have been performed, assuming the complete particle ensemble to consist of STS. The model results show much higher backscatter ratios than the measurements, peaking at values larger than 20 at 940 nm. The good agreement between the model and the backscatter measurements support the assumption that the cloud consists of a large mode of NAT particles, which contains most of the particle volume. The asphericity of the solid particles might be a hint to the NAT formation process. Deposition nucleation of NAT on solid surfaces could lead to nonspherical particle shapes.

[10] The NAT formation process is investigated with a detailed microphysical simulation of a PSC layer detected near 480 K potential temperature at 21.9 h UT and again about 1.2 hours later for 8 min. Figure 4 shows the measured particle volumes versus potential temperature for the ascent and the descent. The shaded area indicates the 480 K PSC particle layer. This layer has been chosen for reference due to its relatively long sampling time, which reduces statistical experimental errors.

4. Microphysical Model Description

[11] The microphysical model [*Larsen et al.*, 2000] describes growth and evaporation of STS particles in equilibrium with the gas phase and applying mass conservation. Additionally, slow homogeneous freezing of NAT (NAD) from STS particles at temperatures above T_{ice}, based on a parameterization of *Tabazadeh et al.* [2001], as well as homogeneous nucleation of ice in STS particles 3–4 K below T_{ice}, based on freezing rates determined by *Koop et al.* [2000] is calculated. The ice evaporates at temperatures above T_{ice} and particles consisting of NAT and SAT (sulfuric acid tetrahydrate) are left behind. NAT evaporates at temperatures above T_{NAT}. The model has been initialized 20 days prior to the measurements at 210 K with a bimodal lognormal sulfate aerosol size distribution of 500 particle size classes as derived from the OPC measurements. The model is run in a Eulerian mode in radius space, which assumes that after growth, evaporation or freezing, a fraction of the particles contained in one size class is transferred to another appropriate particle class. This model setup allows for the simulation of very slow nucleation rates (necessary for homogeneous NAT/NAD nucleation), which

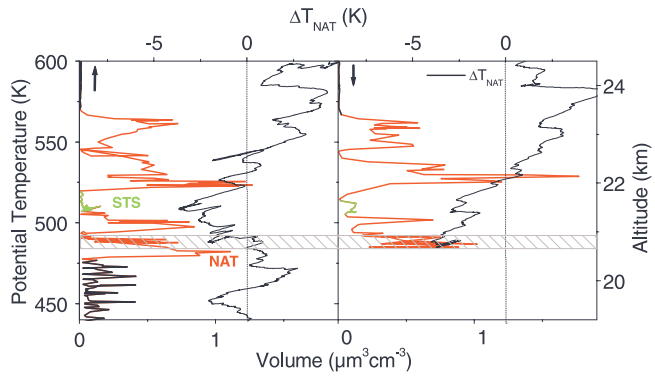

Figure 4. Particle volume and measured temperature difference to T_{NAT} (black line) versus potential temperature for the ascent and the descent of the balloon on 19 January 2000. The shaded area indicates the analyzed 480 K PSC layer.

are not covered in a Lagrangian approach of particle growth in radius space.

5. Trajectory Calculations

[12] The microphysical box model [*Larsen*, 2000] is driven by isentropic temperature histories to simulate PSC formation and measurements on 19 January 2000. Twenty day temperature histories of the air parcels sampled during the balloon flight have been calculated from ECMWF analysis [*Knudsen et al.*, 2001]. The air parcels stayed inside the vortex for the whole period. The analysis shows that the air temperatures between 440 and 560 K potential temperature oscillated between T_{ice}, and T_{NAT} for more than 15 days. After an increase to 200 K, 4 days prior to the encounter the temperatures again dropped, and remained below T_{NAT} approximately 36 hours before the sampling.

[13] A mesoscale MM5 trajectory [*Dörnbrack et al.*, 2002] starting 4 hours prior to the measurements has been appended to the synoptic temperature history at 480 K, as it better covers the temperature oscillations induced by low mountain-wave activity observed on 19 January 2000 over northern Scandinavia. The mesoscale temperature history has been adjusted to the ECMWF analysis and the measured temperatures. The only accepted pathways to NAT formation for particles recently exposed to temperatures above 200 K is through the nucleation of ice. Homogeneous ice freezing in STS critically depends on the temperature and the cooling rate [*Koop et al.*, 2000]. To simulate a partial freezing of the STS population (i.e., freezing of only the large-size end of the size distribution) would require a temperature accuracy of better than 0.1 K [*Larsen et al.*, 2002]. No temperature hindcasts have this accuracy. The lowest temperature calculated with the MM5 model on 19 January 2000 at 20.5 h UT is 0.5 K above that required to induce ice formation in the microphysical model. Since without ice formation, no reasonable agreement between the measurements and the model could be achieved, the lowest MM5 temperatures were lowered by 0.5 K to induce ice freezing.

6. NAT Particle Formation and Properties

[14] The synoptic and mesoscale temperature history at 480 K potential temperature, T_{NAT} and T_{ice} are shown in Figure 5a versus time in hours ending at the measurements on 19 January 2000 at 23.2 h UT. Figure 5b presents the simulated particle evolution in terms of total aerosol volume. Up to 3 hours prior to the measurements (20 h UT), the growth of purely liquid binary and ternary particles is simulated; there is no homogeneous or heterogeneous nucleation of NAT nor ice with particle number densities larger than 10^{-5} cm^{-3}. Homogeneous nucleation of NAT is negligible. Ice starts to freeze in the ternary droplets 3 hours prior to the measurements, and the PSC volume increases to peak values larger than 10 μm^{3}cm^{-3}. After the evaporation of the ice particles, NAT particles are left behind, which take up water and nitric acid and increase in size and volume.

[15] The later part of the simulation starting at 14 h UT is presented in Figure 6. Note the change in timescale at 23 h UT. Figure 6a shows the temperature

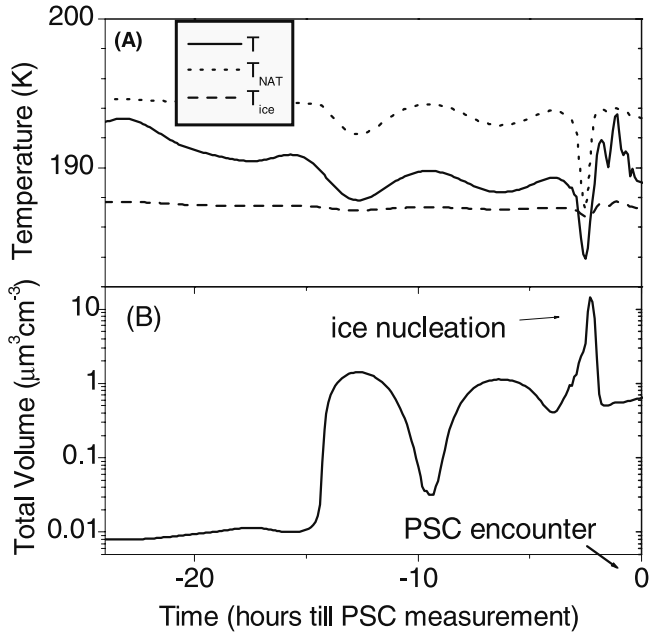

Figure 5. Temperature trajectories ending in the 480 K NAT layer sampled twice on 19 January 2000. Time is in hours prior to the measurements at 23.1 h UT. (a) Simulated temperature history (black line); up to −4 h synoptic temperatures, thereafter mesoscale MM5 temperatures; T_{NAT} (dotted line) and T_{ice} (dashed line) calculated with the measured water vapor, assuming 8 ppbv nitric acid. (b) Simulated total particle volume (black line). The peak in the particle volume 3 hours prior to the measurements indicates ice nucleation.

history (black line) and the frost point temperature (blue line) compared to the measurements (black and blue squares). Total and gas phase water, nitric and sulfuric acid are shown in Figure 6b. The other panels compare the measurements (symbols) with calculated properties (lines) in terms of integrated particle number density of different particles size classes with radii larger than 0.15 μm (Figure 6c), total particle volume (Figure 6d), median radii of NAT and liquid particles (Figure 6e), and composition in terms of water to nitric acid mole ratio or acid weight fraction (Figure 6f). There is reasonable agreement between the model and measurements at 21.9 h UT and near 23.1 h UT. The simulated particle properties of the 480 K potential temperature layer can be explained in terms of NAT particles with volumes between 0.5 and 0.6 μm^{3}cm^{-3}, median radii near 1 μm and number densities near 0.04 cm^{-3}. NAT clouds with those properties have previously been labeled type 1a. A small fraction of the particles is STS and contains less than a tenth of the total aerosol volume. The simulation clearly shows that a potential formation mechanism of the NAT particles is NAT nucleation on ice particles, accepting the temperature adjustment applied to the mesoscale model temperatures.

[16] Sensitivity studies have been performed using 6 and 10 ppbv nitric acid for the model calculations. The model results (gray shaded area) are compared to the particle size distribution measured at 480 K at 23.1 h UT

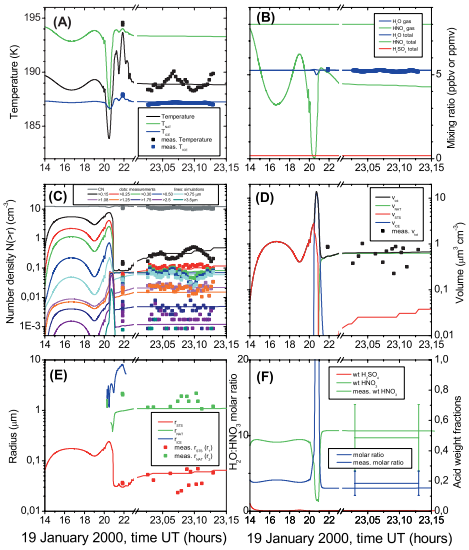

Figure 6. Evolution of PSC particle properties from 14 h UT to 23.15 h UT on 19 January 2000; comparison of measurements (squares) with model results (lines). Time is given in decimal hours. After 23 h the timescale is expanded to show 8 min of observations between 23.0 and 23.13 h. (a) Temperature (black line) compared to the measured temperature (squares), T_{NAT} (green line) and T_{ice} (blue line), measured T_{ice} (blue squares). (b) Total and gas phase nitric acid (green lines), sulfuric acid (red line), water vapor and total water (blue lines) compared to the measured water vapor (blue squares). (c) Simulated integrated particle number density for different size classes N(>r) (lines) compared to the measurements (squares). (d) Total particle volume (black squares and line), volume of NAT (green), STS (red) and ice particles (blue line). (e) Median radius of NAT (green line), STS (red line) and ice particles (blue line) compared to the measurements (squares). (f) H_2O/HNO_3 molar ratio compared to the measurements (blue line with error bars), nitric acid (green line) and sulfuric acid (red line) weight fractions, compared to the measurements (green line with error bars).

in Figure 7. Whereas the small liquid particles increase in volume at higher nitric acid partial pressures, the particle size distribution of the larger NAT particles shows only small differences.

[17] In the following, we discuss the issue of particle sedimentation. We distinguish between sedimentation of large nitric acid containing particles ($r \approx 5$ μm), colloquially called NAT rocks [*Fahey et al.*, 2001], into the mountain-wave PSC and sedimentation of the observed smaller NAT particles.

[18] A microphysical simulation has been performed allowing for the sedimentation of NAT and ice out of a 1 km thick layer at 480 K potential temperature. The largest measured NAT particles have radii of 4 μm. They probably have formed 3 hours prior to the measurements. A 4 μm NAT particle sediments approximately 50 m in 3 hours. Therefore the particle size distributions simulated at 23.1 h UT show only minor differences and sedimentation of the mountain-wave NAT particles is negligible as shown in Figure 7 (dotted line).

[19] ECMWF data show large-scale low temperatures and trajectories with temperatures below T_{NAT} for more than 2 weeks. Therefore we investigate the sedimentation of large NAT particles which might have formed in the cold period into the observed mountain-wave PSC. Those large NAT particles have particle number densities below the detection limit of the OPC ($5 * 10^{-4}$cm^{-3}). Additional simulations have been performed on ECMWF trajectories at higher altitudes (between 480 and 560 K in steps of 20 K). Those trajectories also show temperature maxima 4 to 7 K above T_{NAT} for more than 24 hours 3 to 4 days prior to the measurements. At those high temperatures any previously formed NAT particles would evaporate and NAT rock sedimentation from the previous 15 day cold temperature period into the measured PSC is not possible.

7. Comparison of Mountain-Wave PSC Data on 19 and 25 January 2000

[20] On 19 January 2000, air parcel histories were located clearly inside the vortex for the previous 20 days with temperatures below T_{NAT} for more than two weeks. Five to six days prior to sampling the temperature increased and remained above 200 K for two days. The temperature then decreased below T_{NAT} approximately 36 hours prior to the measurements. The NAT particle volumes in the lee waves generally were between 0.5 and 1 μm^{3}cm^{-3}, which might give hints of denitrification inside the vortex.

[21] In contrast, on 25 January 2000 NAT particle volumes were larger, between 1 and 3 μm^{3}cm^{-3} [*Voigt et al.*, 2000a; *Schreiner et al.*, 2002]. In this case, the synoptic trajectories were located closer to the edge of the vortex and the air did not experience temperatures below T_{NAT} for weeks. Similarly to 19 January, the temperatures also dropped below T_{NAT} approximately one day prior to the measurements. For 25 January the microphysical model

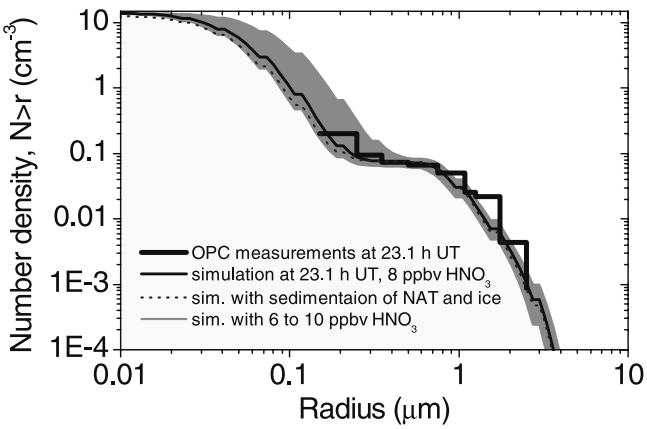

Figure 7. Measured (thick black line) and simulated (thin black line) integrated particle number density N(>r) on 19 January 2000 at 23.1 h UT. The simulations use measured water and sulfuric acid and assume 8 ppbv nitric acid. Simulations with sedimentation of NAT and ice (dotted line) and simulations with 6 to 10 ppbv nitric acid (gray shaded area) are also shown.

calculations are in agreement with the measurements assuming a nitric acid mixing ratio of 14 ppbv [*Larsen et al.*, 2002] and 8 ppbv is required for 19 January 2000. The differences in the particle volumes can be explained by differences in the nitric acid partial pressure, which can be caused by denitrification inside the vortex. Denitrification can be less severe at the edge of the vortex, where generally temperatures are higher due to entrainment of extra-vortex air and increasing times of sunlight.

[22] Although the PSC volumes in the two cases show some differences, NAT could have nucleated on ice in both cases. The ice has formed in a mountain-wave event above the Scandinavian mountains, and the timescales for NAT growth for both PSC events are approximately 3 hours. Measured NAT particle size distributions are similar with median radii between 1 and 2 μm on 19 January and between 0.5 and 1.5 μm on the 25th. In both flights, the largest observed particles have radii of 4 μm at number densities larger than $5 * 10^{-4}$ cm^{-3}. In contrast, the measured particle number densities for the NAT particle mode are clearly different. On 25 January, they are about an order of magnitude higher compared to 19 January 2000. The optical particle counter also measured the number density of condensation nuclei. On 19 January 2000, CN number densities are on the average 12 cm^{-3} and NAT number densities are between 0.01 and 0.2 cm^{-3}. On 25 January similar CN number densities (15 cm^{-3}), but higher NAT number densities between 0.2 and 2 cm^{-3} were detected. From these data, the fractions of CN on which NAT nucleated can easily be calculated. Microphysical modeling suggests that NAT has formed on ice in both cases. Ice nucleation rates measured by *Koop et al.* [2000] suggest complete ice activation at cooling rates larger than 10 K/h. Lower cooling rates lead to selective ice nucleation. Assuming complete ice activation, NAT formed on a fraction of 0.1 to 2% of the ice particles on 19 January and on a larger fraction (1 to 13%) of the ice particles in the mountain-wave event six days later.

[23] The NAT particle fractions or NAT particle number densities can be related to the strength of the rising motion in the mountain-wave cloud, expressed in terms of the cooling rate. The cooling rate for both PSCs has been determined from the mesoscale MM5 model, which has large uncertainties and only a trend can be given. For 19 January the cooling rate ranged between 5 and 15 K/h. On 25 January the cooling rate was higher, between 10 and 50 K/h. Higher cooling rates lead to higher NAT supersaturations, caused by nonequilibrium in the nitric acid/water uptake by particles. The measurements show that higher cooling rates or stronger wave activity in the stratosphere can cause NAT nucleation on a larger fraction of the ice particles and higher NAT particle number densities in mountain-wave clouds.

8. Summary

[24] On 19 January 2000, polar stratospheric clouds have been observed with multiple instruments on a balloon flight. The measured optical and microphysical particle properties as well as optical model results indicate that a large fraction of the particles are NAT. Microphysical modeling of chemical and physical particle properties measured in a cloud layer near 480 K shows that this NAT particle layer could have formed on ice if the modeled mesoscale temperatures are reduced by 0.5 K. A similar NAT formation process has been derived for the NAT PSC layers observed on 25 January 2000 [*Larsen et al.*, 2002]. We suggest that differences in measured NAT particle number densities on 19 and 25 January could result from different meteorological conditions, under which those particles formed. On 25 January stronger wave activity with faster rising motion and therefore larger cooling rates can lead to higher NAT particle number densities compared to the NAT cloud observations on 19 January. Particle processing during temperature changes induced by mountain waves have a great impact on PSC properties. High NAT particle number densities as observed in both mountain-wave PSCs enhance chlorine activation as prerequisite for strong ozone destruction.

[25] **Acknowledgments.** The balloon flights were performed as part of the European-American SOLVE/THESEO 2000 campaign in winter 1999/2000. We thank CNES for the excellent balloon support. This work has been supported by the Commission of the European Union through the Environment and Climate Program (contract ENV4-CT97-0523) and through the CIPA program (EVK2-CT-2000-00095). The work of T.D. and C.K. has been supported by the U.S. National Science Foundation. ECMWF is thanked for the provision of their analysis. We want to thank the reviewer for the comments.

References

Adriani, A., F. Cairo, S. Mandolini, G. Di Donfrancesco, T. Deshler, and B. Nardi, A new joint balloon-borne experiment to study polar stratospheric clouds: Laser backscatter sonde and optical particle counter, in *Atmospheric Ozone: Proceedings of XVIII Quadriennial Ozone Symposium*, vol. 2, edited by R. D. Bojkov and G. Visconti, pp. 879–882, Edigrafital for Parco Sci. e Tecnol. d'Abruzzo, Italy, 1998.

Carslaw, K. S., et al., Stratospheric aerosol growth and HNO_3 gas phase depletion from coupled HNO_3 and water uptake by liquid particles, *Geophys. Res. Lett.*, *21*, 2479–2482, 1994.

Deshler, T., B. Nardi, A. Adriani, F. Cairo, G. Hansen, F. Fierli, A. Hauchecorne, and L. Pulvirenti, Determining the index of refraction of polar stratospheric clouds above Andoya by combining size resolved concentration and optical scattering measurements, *J. Geophys. Res.*, *105*, 3943–3953, 2000.

Dhaniyala, S., K. A. Mckinney, and P. O. Wennberg, Lee-wave clouds and denitrification of the polar stratosphere, *Geophys. Res. Lett.*, *29*, 1322, doi:10.1029/2001GL013900, 2002.

Dörnbrack, A., T. Birner, A. Fix, H. Fientje, A. Meister, H. Schmid, E. V. Browell, and M. J. Mahoney, Evidence for inertia gravity waves forming polar stratospheric clouds over Scandinavia, *J. Geophys. Res.*, *107*(D20), 8287, doi:10.1029/2001JD000452, 2002.

Fahey, D. W., et al., The detection of large HNO_3 particles in the winter Arctic stratosphere, *Science*, *291*, 1026–1031, 2001.

Fueglistaler, S., B. P. Luo, C. Voigt, K. Carslaw, and T. Peter, NAT-rock formation by mother clouds: A microphysical model study, *Atmos. Chem. Phys. Discuss.*, *2*, 29–42, 2002.

Hanson, D. R., and A. R. Ravishankara, Reaction of $ClONO_2$ with HCl on NAT, NAD, and frozen sulfuric acid and hydrolysis of N_2O_5 and $ClONO_2$ on frozen sulfuric acid, *J. Geophys. Res.*, *98*, 22,931–22,936, 1993.

Knudsen, B. M., J.-P. Pommereau, A. Garnier, M. Nunes-Pinharanda, L. Denis, G. Letrenne, M. Durand, and J. M. Rosen, Comparison of stratospheric air parcel trajectories based on different meteorological analyses, *J. Geophys. Res.*, *106*, 3415–3424, 2001.

Koop, T., B. P. Luo, A. Tsias, and T. Peter, Water activity as determinant for homogeneous ice nucleation in aqueous solutions, *Nature*, *406*, 611–614, 2000.

Krieger, U. K., J. C. Mossinger, B. P. Luo, U. Weers, and T. Peter, The measurement on the refractive indices of H_2SO_4–HNO_3–H_2O solutions to stratospheric temperatures, *Appl. Opt.*, *39*, 3691–3703, 2000.

Larsen, N., Polar stratospheric clouds: Microphysical and optical models, *Sci. Rep. 00-06*, Dan. Meteorol. Inst., Copenhagen, 2000.

Larsen, N., et al., Microphysical mesoscale simulations of polar stratospheric cloud formation constrained by in situ measurements of chemical

and optical cloud properties, *J. Geophys. Res.*, *107*(D20), 8301, doi:10.1029/2001JD000999, 2002.
Mishchenko, M., Light scattering by randomly orientated axially symmetrical particles, *J. Opt. Soc. Am.*, *8*, 871–882, 1991.
Ovarlez, J., and H. Ovarlez, *Stratospheric water vapor content evolution during EASOE*, *21*, 1235–1238, 1994.
Rosen, J. M., and N. T. Kjome, Backscattersonde: A new instrument for atmospheric aerosol research, *Appl. Opt.*, *30*, 1552–1561, 1991.
Schreiner, J., et al., Chemical analysis of polar stratospheric cloud particles, *Science*, *283*, 968–970, 1999.
Schreiner, J., et al., Chemical, microphysical, and optical properties of polar stratospheric clouds, *J. Geophys. Res.*, *107*, 8313, doi:10.1029/2001 JD000825, 2002 [printed *108*(D5), 2003].
Solomon, S., R. R. Garcia, F. S. Rowland, and D. J. Wuebbles, On the depletion of Antarctic ozone, *Nature*, *321*, 755–758, 1986.
Tabazadeh, A., E. J. Jensen, O. B. Toon, K. Drdla, and M. R. Schoeberl, Role of the polar stratospheric freezing belt in denitrification, *Science*, *291*, 2591–2594, 2001.
Voigt, C., et al., NAT in polar stratospheric clouds, *Science*, *290*, 1756–1758, 2000a.
Voigt, C., S. Tsias, A. Dörnbrack, S. Meilinger, B. P. Luo, J. Schreiner, N. Larsen, K. Mauersberger, and T. Peter, Non-equilibrium compositions of liquid polar stratospheric clouds in gravity waves, *Geophys. Res. Lett.*, *27*, 3873–3876, 2000b.
Waibel, A., T. Peter, K. S. Carslaw, H. Oelhaf, G. Wentzel, P. J. Crutzen, U. Pöschl, A. Tsias, E. Reimer, and H. Fischer, Arctic ozone loss due to denitrification, *Science*, *283*, 2064–2069, 1999.
Worsnop, D., et al., Vapour pressures of solid hydrates of nitric acid: Implication for polar stratospheric clouds, *Science*, *259*, 71–74, 1993.

A. Adriani, F. Cairo, and G. Di Donfrancesco, Istituto per la Scienza dell'Atmosfera e del Clima, Sezione di Roma, Via Fosso del Cavaliere 100, I-00133 Rome, Italy. (a.adriani@isac.cnr.it; f.cairo@isac.cnr.it; didonfra@ifa.rm.cnr.it)

T. Deshler, C. Kröger, and J. Rosen, University of Wyoming, Department of Atmospheric Science, P.O. Box 3038, Laramie, WY 82071, USA. (deshler@uwyo.edu; ckroger@uwyo.edu)

A. Dörnbrack and C. Voigt, Institut für Physik der Atmosphäre, DLR Oberpfaffenhofen, D-82234 Wessling, Germany. (andreas.doernbrack@dlr.de; christiane.voigt@dlr.de)

B. M. Knudsen and N. Larsen, Danish Meteorological Institute, Division of Middle Atmospheric Research, Lyngbyvej100, DK-2100 Copenhagen, Denmark. (nl@dmi.dk)

B. Luo, Eidgenössische Technische Hochschule, Institut für Atmosphäre und Klima (IACETH), HPP, Ch-8093 Zürich, Switzerland. (luo@atmos.umnw.ethz.ch)

K. Mauersberger and J. Schreiner, Max-Planck-Institute for Nuclear Physics, Division of Atmospheric Physics, P.O. Box 103980, D-69029 Heidelberg, Germany. (Konrad.Mauersberger@mpi-hd.mpg.de; Jochen.Schreiner@mpi-hd.mpg.de)

H. Ovarlez and J. Ovarlez, Laboratoire de Meteorologie Dynamique, UMR 8539, F-91128 Palaiseau, France. (joelle.ovarlez@polytechnique.fr)